



Title	Deformation and Bond-Area Expansion of Thick Aluminum Wire during Ultrasonic Bonding
Author(s)	Maeda, Masakatsu; Takahashi, Yasuo
Citation	Transactions of JWRI. 2013, 42(2), p. 15-20
Version Type	VoR
URL	https://doi.org/10.18910/27403
rights	
Note	

The University of Osaka Institutional Knowledge Archive : OUKA

<https://ir.library.osaka-u.ac.jp/>

The University of Osaka

Deformation and Bond-Area Expansion of Thick Aluminum Wire during Ultrasonic Bonding[†]

MAEDA Masakatsu*, TAKAHASHI Yasuo**

Abstract

Thick Al wires were welded with Al-Si, Si and SiO₂ substrates by ultrasonic bonding to investigate the deformation and the bond-area expansion behavior simultaneously in detail with a high-speed measuring system. The deformation of the wire by the application of the bonding force is completed immediately. The deformation restarts by the application of the ultrasonic vibration. The deformation induced by applying the bonding force consists of only an elastic component, whereas that by ultrasonic vibration consists of only a plastic component. The Al wire is not work-hardened by the plastic deformation during application of ultrasonic vibration. The adhered area expands in the direction perpendicular to the ultrasonic vibration. The evolution of the wire deformation behavior and the expansion of the adhered area show an intimate correlation with each other.

KEY WORDS: (High-speed process monitoring), (Deformation of wiring material), (Expansion of adhered area), (Ultrasonic wedge bonding), (Power electronic devices)

1. Introduction

Ultrasonic bonding is one of the solid-state welding techniques widely applied in electronics packaging for connecting wiring materials to pads on semiconductor chips and to outer-circuits¹⁻⁵⁾. The technique forms solder-free direct interconnections at low temperature and within a very short time¹⁾. Thus, sound interconnections formed by ultrasonic bonding perform with high reliability at high temperatures. This feature makes the technique irreplaceable for wiring electronic devices used at high temperatures and under high thermal cycle conditions, *e.g.*, heavy-duty power electronics. Power electronics is becoming more important than ever as one of the key technologies to improve energy efficiency of electric systems. Application fields of power electronics are broadening rapidly. Furthermore, the demands on them are getting severer. To fulfill the demands, the wires are becoming thicker. On the other hand, each interconnection must guarantee extremely high reliability, since only one failure in the connections can halt the entire system. To achieve such a high reliability in manufacturing, *in-situ* monitoring of the bonding processes and rapid feeding back of the judgments about the processes are required⁶⁻⁸⁾. Therefore, correct understanding on the phenomena occurring at the bond interface during ultrasonic bonding is required for precise control of the process.

Several approaches to the ultrasonic bonding mechanism have been reported. Harman and Albers reported that the adhesion always initiates around the perimeter of the surfaces in contact¹⁾. Their results indicate that the frictional sliding occurs only at the periphery, instead of the entire contact area. Lum et al. investigated the adhesion behavior between Au⁴⁾ or Al⁵⁾ wires and Cu substrates and proposed a model which describes the ratio of sliding and stationary area. Their model predicts that the entire interface sliding is achieved by setting the bonding parameters with low bonding force and high ultrasonic power as a function of the static friction coefficient of the interface. Shah et al. implemented *in-situ* measurement of shear force applied in the vicinity of a bonding pad during ultrasonic bonding and derived the ultrasonic friction power⁸⁾. Their results showing four stages of interfacial sliding provide a clear insight of ultrasonic bonding behavior. However, knowledge of the interfacial phenomena based on such *in-situ* measurement is still insufficient for understanding and controlling the bonding process.

The present study has been implemented to elucidate the contact area expansion behavior induced by deformation of thick Al wire during ultrasonic bonding using high-speed measurement and observation techniques: a 2560 kHz laser-Doppler vibrometer, a 50 kHz laser displacement sensor and a high-speed video

† Received on September 30, 2013

* Assistant Professor

** Professor

Transactions of JWRI is published by Joining and Welding Research Institute, Osaka University, Ibaraki, Osaka 567-0047, Japan

microscope.

2. Experimental procedure

The ultrasonic bonding apparatus prepared for the present study is schematically illustrated in **Fig. 1**. The apparatus was equipped with a 60 kHz ultrasonic transducer, a linear motor for applying various bonding forces, a laser-Doppler vibrometer, a laser displacement sensor, and a high-speed digital video camera. The wedge tool attached to the transducer was made of cemented carbide and had a V-grooved chucking face. The wedge tool holds a wire by applying the bonding force perpendicular to the wire axis. The laser-Doppler vibrometer monitored the ultrasonic vibration behavior at the tip of the wedge-tool with the sampling rate of 2560 kHz. Unfortunately, the amplitude of vibration at the interface between the wire and substrate was quite difficult to monitor. Although the amplitude at the interface is known to be lower than that at the tip of the wedge tool, the position was selected as the monitorable position at which the vibration behavior is in the closest relation with that at the interface. The laser displacement sensor measured the displacement of the wedge tool in a direction perpendicular to the bond interface with the sampling rate of 100 kHz. Since the wedge tool is sufficiently rigid, the displacement can be related solely to the change in the height of the wire. The deformation of the wire is represented by this value. It should be noted that, however, the actual elastic or plastic strain at each part of the wire is not homogeneous. The high-speed video microscope observed the expansion behavior of the adhered area from the back of the substrate with a frame rate of 1000 fps (1 kHz). Thus, a cumulative photogene of 60-cycles-motion was recorded on one frame of the video. The frame rate was obviously insufficient. Unfortunately, it was the highest at this moment with a good image resolution to analyze the adhered area.

In general wire bonding, fully annealed wires are used in order to enhance the expansion of the adhered area and to suppress the damage of the semiconductor substrates. In the present study, on the contrary, as-drawn (*i.e.*, work-hardened) Al wires of which diameter and nominal purity were 300 μm and 99.9 %, respectively, were used in order to slow down the deformation behavior of the wire to a level detectable with the measuring systems described above. On the other hand, three types of substrates were prepared, namely Al-Si, SiO_2 and Si substrates. The Al-Si substrates were 1.5- μm -thick Al-1 mass%Si alloy films deposited on 0.6-mm-thick Si substrates, which are similar to pads on power electronic devices. The SiO_2 substrates were high-purity SiO_2 glass disks of which diameter and thickness were 20.91 mm and 3.00 mm, respectively. They were employed to make it possible to observe the adhesion behavior at the interface from the back of the substrates. The Si substrates were 1.00-mm-thick Si single-crystal chips cut into a size of 5.0-mm-square. The substrates were first used in the preliminary study, since the surfaces of both SiO_2 and Si substrates consist of SiO_2 . Although the

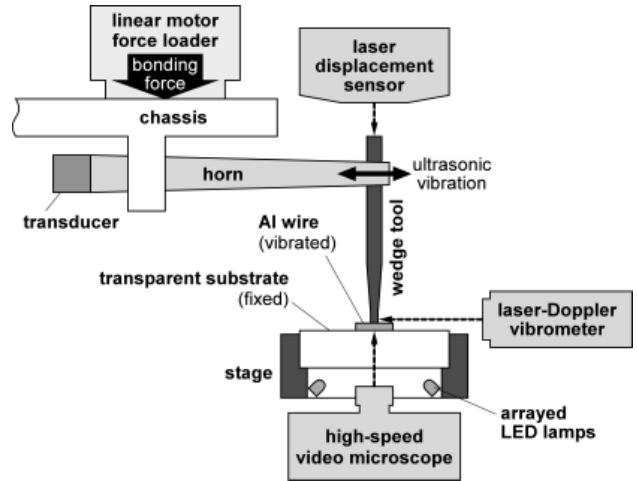


Fig. 1 Schematic illustration of the ultrasonic bonding apparatus used in the present study.

combination of Al wire and SiO_2 substrate is different from that of practical wire and electrode-pad on a semiconductor chip, the deformation of the wire and expansion of adhered area during the ultrasonic bonding process will be fundamentally the same. Therefore, the knowledge to predict and control the deformation behavior of wire in practical combination of materials can be obtained by measuring the behavior of those employed in the present study.

Bonding experiment was implemented in ambient temperature and atmosphere using a bonding sequence described in **Fig. 2**. A constant bonding force in the range from 1.0 to 7.0 N was applied to the wire at first. The wire was kept pressed on the substrate for 300 ms to damp the vibration generated by the impact of the bonding force. Then, the ultrasonic vibration was applied for 200 ms. The ultrasonic power was set at a constant value between 0.25 and 3.0 W. Finally, the bonding force was unloaded 1000 ms after finishing the application of the ultrasonic vibration. This long holding time was introduced to homogenize the temperature distribution in the wire caused by application of ultrasonic vibration.

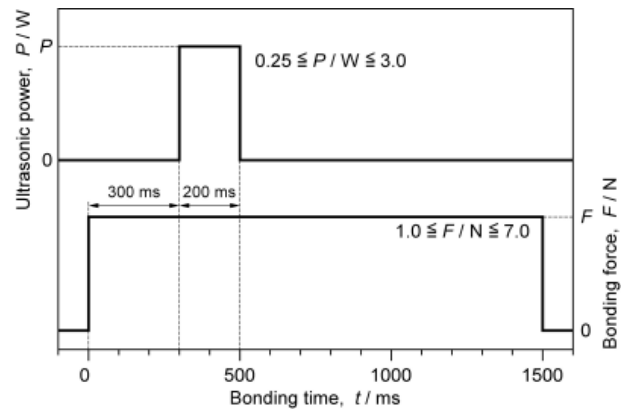


Fig. 2 Ultrasonic bonding sequence adopted in the present study.

The changes in the vibration behavior, wire height, and bond area were monitored with the laser Doppler vibrometer, laser displacement sensor, and high-speed video microscope, respectively, throughout the bonding operation.

3. Results and discussion

Fig. 3 shows a typical displacement behavior of the wedge tool to the direction perpendicular to the bond interface during ultrasonic bonding of Al wire to Si substrate under the ultrasonic power and the bonding force of 2.0 W and 3.0 N, respectively. The wedge-tool moves immediately toward the substrate for Δz_F by applying the bonding force. The displacement does not proceed further after achieving Δz_F , *i.e.*, the wedge-tool is kept at a constant position until the ultrasonic vibration is applied. By applying the ultrasonic vibration, the displacement of the wedge-tool restarts. The displacement rate is high in the beginning and gradually falls. The displacement stops after achieving Δz_{U}^{\max} ($= \Delta z_F + \Delta z_U$) even if the ultrasonic vibration is still applied. In some bonding conditions with short application time of ultrasonic vibration, ultrasonic vibration ends before the deformation saturates. In such cases, the displacement stops at the time ultrasonic vibrations end. At the end of ultrasonic vibration, the wedge-tool does not spring back toward the balancing point with the bonding force ($z = \Delta z_F$). This phenomenon indicates that the displacement induced by ultrasonic vibration (Δz_U) consists of only plastic deformation of the wire, *i.e.*, it does not contain an elastic component. This deformation behavior is clearly different from that which occurs by increasing static bonding force. When the bonding force is unloaded, the wedge tool springs back for Δz_E . The value of Δz_E corresponds to the elastic component of deformation conserved in the wire after the application of ultrasonic vibration.

Fig. 4 shows the dependence of Δz_F , Δz_U and Δz_E on

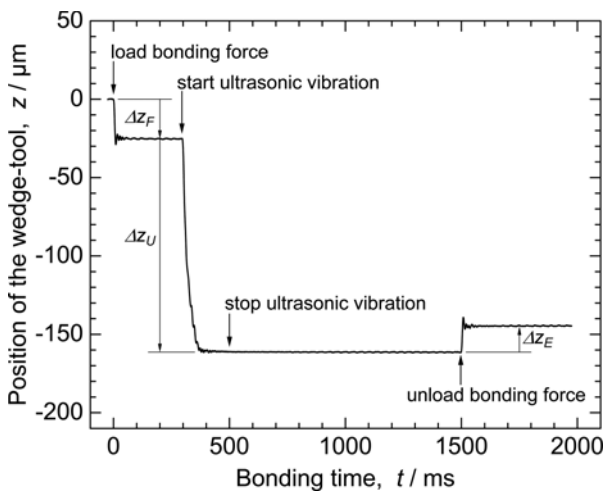


Fig. 3 Displacement behavior of wedge-tool during ultrasonic bonding of Al wire to Si substrate under the condition of 2.0 W, 3.0 N.

the bonding force at a constant ultrasonic power of 1.0 W. The absolute values of Δz_F and Δz_E increase proportionately with the bonding force, obeying the Hooke's law. Thus, the deformation behaviors at these stages consist of elastic components. On the other hand, the absolute value of Δz_U increases at first and then turns to decrease by increasing the bonding force, showing a maximum deformation (Δz_U^{\max}) at 3.0 N. Although the amplitude of ultrasonic vibration will be large at a condition with a low bonding force, the frictional force applied to the wire and the substrate by ultrasonic scrubbing is weak. Thus, it will require a long time to remove the bond-preventing surface layer and to form an initial adhesion, which is required for macroscopic wire deformation by folding. At a condition with a high bonding force, the frictional force will be large enough to remove the bond-preventing layer. However, the large frictional force also constrains the scrub motion. To form

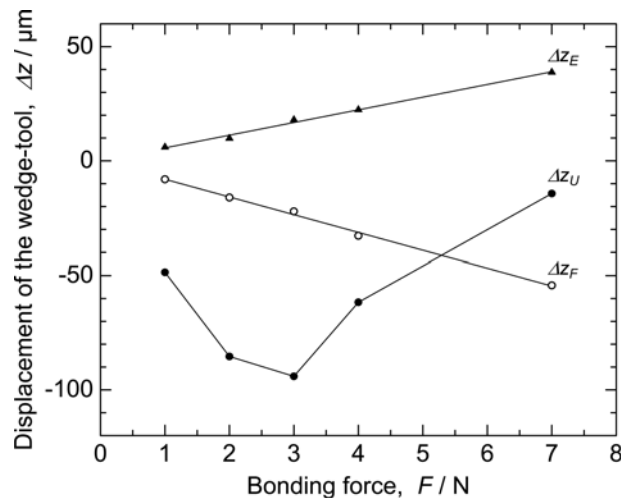


Fig. 4 Change in Δz_F , Δz_U and Δz_E with ultrasonic power at a constant bonding force of 3.0 N.

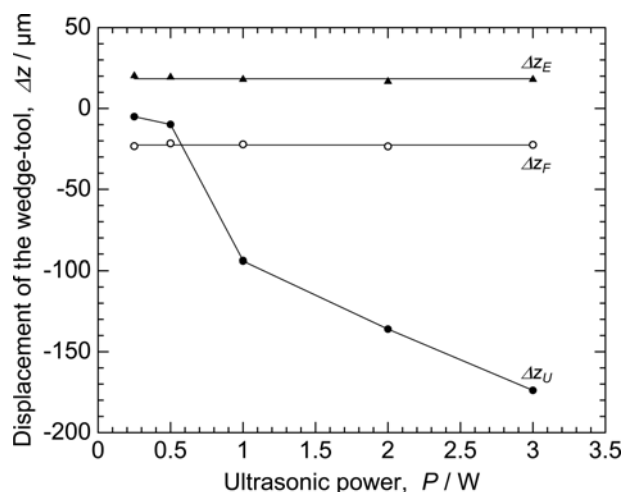


Fig. 5 Change in Δz_F , Δz_U and Δz_E with bonding force at a constant ultrasonic power of 1.0 W.

an initial adhesion, the newly exposed surfaces have to be moved for a certain distance to meet with the fresh surface on the counter side. Therefore, the suppression of vibration amplitude will suppress the probability of formation of the initial adhesion. The condition at which $\Delta z_{\text{U}}^{\text{max}}$ is achieved will correspond to the boundary of microslip and gross-sliding proposed by Lum et al.⁵⁾, since the condition satisfies both the strong frictional force and large frictional motion simultaneously. The bonding force has an optimum value which depends on the ultrasonic power to be applied.

Fig. 5 shows the dependence of Δz_{F} , Δz_{U} and Δz_{E} on the ultrasonic power at a constant bonding force of 3.0 N. It is clearly seen that Δz_{F} and Δz_{E} appear constant at every ultrasonic power investigated, whereas Δz_{U} increases by increasing the ultrasonic power. It is easily understood that Δz_{F} is constant under a constant bonding force. The change of Δz_{U} depending on the ultrasonic power, showing the transition from microslip to gross-sliding at the ultrasonic power between 0.5 and 1.0 W, is also an expected behavior as explained above. On the other hand, Δz_{E} was expected to change depending on the work-hardening of the wire induced by plastic deformation during ultrasonic vibration (Δz_{U}). This result implies that the wire is not work-hardened by the deformation of Δz_{U} .

It is revealed that Δz_{U} consists of only plastic component which is not accompanied by work-hardening. The temperature change of the wire during ultrasonic bonding has to be taken into consideration to understand why the Al wire is not work-hardened. The wire is heated by friction and plastic deformation during applying the ultrasonic vibration. An evidence of the temperature change is observed in Fig. 4. The absolute value of the gradient of Δz_{F} appears larger than that of Δz_{E} . The gradients of Δz_{F} and Δz_{E} collaterally indicate the elastic modulus of the Al wire before and after applying the ultrasonic vibration, respectively. Therefore, the difference in these two gradients imply the change in the elastic modulus by heating during applying the ultrasonic vibration. Although the peak temperature of the wire in the vicinity of the interface may change depending on the bonding force, unloading the bonding force one second after finishing the application of ultrasonic vibration gives the Al wire an enough time to homogenize and to converge the temperature into a similar value slightly higher than the room temperature. Due to this temperature conversion, the dependence of Δz_{E} on the bonding force appears proportional.

Fig. 6 shows the displacement behavior of the wedge tool during ultrasonic bonding of Al wire to SiO_2 substrate under the condition of 2.0 W, 3.0 N. The behavior appears almost the same with that shown in Fig. 3 except for one point. The spring back of the wedge-tool by unloading the bonding force (Δz_{E}) in the case of the SiO_2 substrate is obviously lower than that of the Si substrate. It should be noted that the surface of Si substrate is covered by a native oxide layer, *i.e.*, amorphous SiO_2 . Therefore, the chemical interaction of

the substrates with the Al wire will be the same. In addition, the surface roughness of SiO_2 substrates is similar to that of Si substrates. Similarities in these points appear in the deformation behavior of the Al wire as the similar values of Δz_{F} and Δz_{U} . On the other hand, the difference in Δz_{E} corresponds to the elastic strain remaining in the Al wire after application of ultrasonic vibration. Since the thermal conductivity of SiO_2 is lower than that of Si by two orders of magnitude, the Al wire is heated to a higher temperature. Due to this effect, the value of Δz_{E} in the case of the SiO_2 substrate is suppressed.

Fig. 7 shows the displacement behavior of the wedge tool during ultrasonic bonding of Al wire to Al-Si substrate under the same condition with that shown in Fig. 6. It is clearly observed that the behavior is similar also in

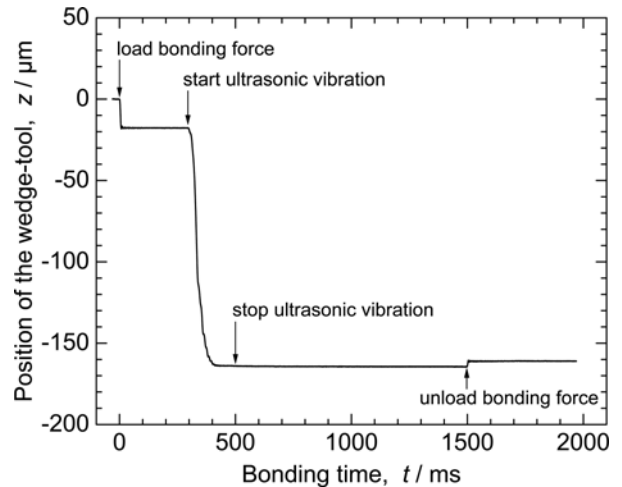


Fig. 6 Displacement behavior of wedge-tool during ultrasonic bonding of Al wire to SiO_2 substrate under the condition of 2.0 W, 3.0 N.

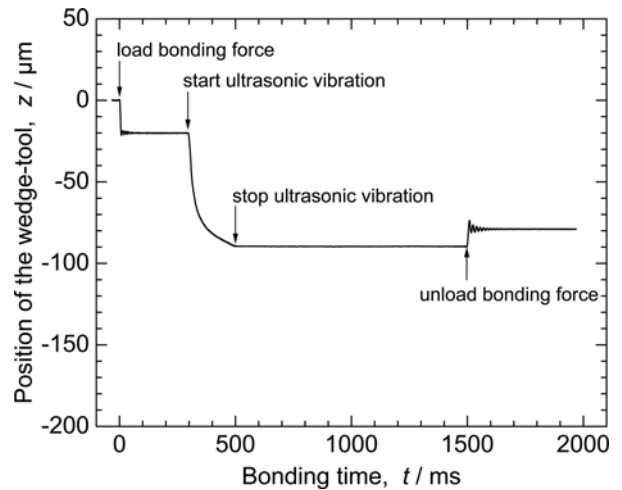


Fig. 7 Displacement behavior of wedge-tool during ultrasonic bonding of Al wire to Al-Si substrate under the condition of 2.0 W, 3.0 N.

the case of Al-Si substrate. By changing the substrate from Si to Al-Si, two points appear different. One is that the wire deformation during applying ultrasonic vibration is not saturated within the time of 200 ms. The other point is that the value of Δz_U is significantly low in the case of Al-Si substrate. These facts indicate that the deformation of the Al wire proceeds slowly when the Al-Si substrate is used. To understand the differences appearing in the deformation behavior of the wire by changing the substrate material, the differences in surface state and deformability (hardness) between Al-Si and Si substrates has to be considered. The surface of Al-Si substrates are rough compared to Si, and covered by amorphous Al_2O_3 which is more chemically stable than SiO_2 . These factors make the adhesion difficult. On the other hand, the Al-Si substrate is softer than Si substrate. This factor will have both positive and negative effects on the adhesion behavior. To break the bond-preventing layer covering the surface of the substrate will be easy. However, the surface of the Al-Si substrate will be dragged by the ultrasonic motion of the wire, *i.e.*, the relative sliding amplitude between the wire and the substrate will be suppressed. Although the easy breakage of the bond-preventing layer can compensate the difficulty of adhesion caused by the surface state of Al-Si substrate, the suppression of the relative sliding amplitude will play the key role in slowing down the deformation rate.

Fig. 8 shows the expansion behavior of the adhered area during ultrasonic bonding of Al wire to SiO_2 substrate under the condition of 1.0 W, 3.0 N. The interface at seven representative stages in the ultrasonic bonding process observed from the back of the SiO_2 substrate.

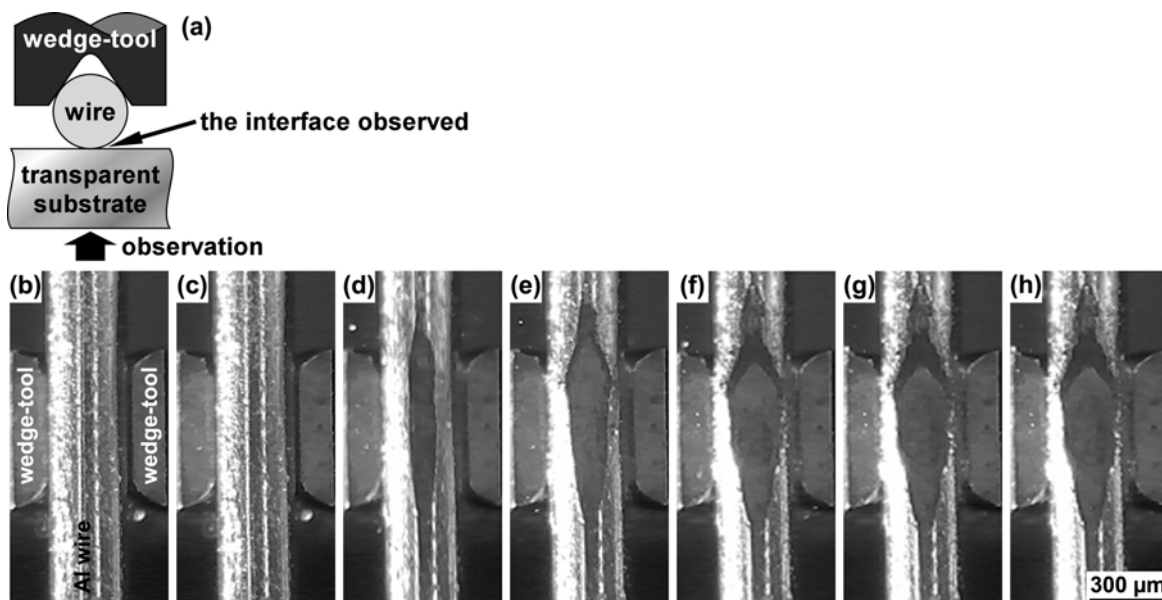


Fig. 8 Change in the shape of the contact area during ultrasonic bonding of Al wire to SiO_2 substrate under the condition of 1.0 W, 3.0 N. The interface was observed from the back of the SiO_2 substrate as schematically illustrated in (a). The states at which (b) before bonding, (c) after the initial bonding force is applied, (d) the ultrasonic vibration is applied for 10 ms, (e) 50 ms, (f) 150 ms, (g) the bonding force is still applied after finishing the application of the ultrasonic vibration and (h) the bonding force is removed are shown.

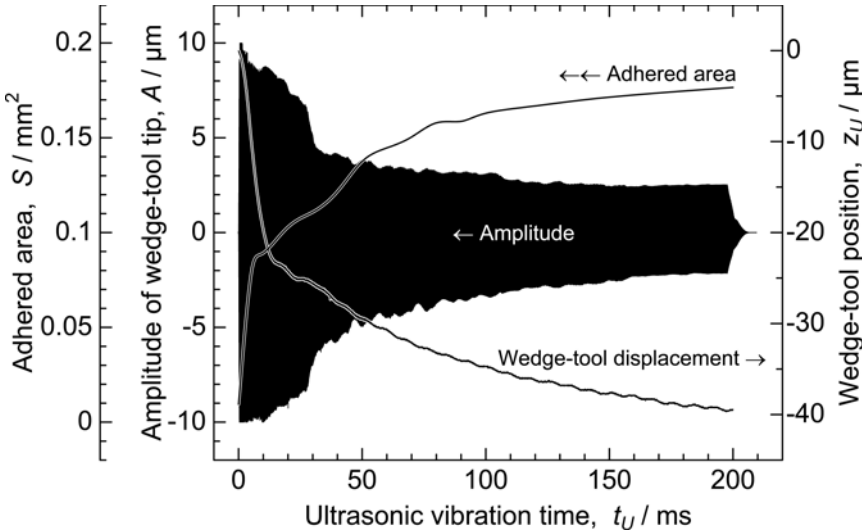


Fig. 9 Relationship among the amplitude at the wedge-tool tip, the displacement of the wedge-tool, and the expansion of the adhered area during ultrasonic bonding of Al wire with SiO_2 substrate under the condition of 1.0 W, 3.0 N.

application of ultrasonic vibration and unloading the bonding force, respectively. The adhered area does not change during these operations of ultrasonic bonding. A decrease of the adhered area might be expected after unloading the bonding force, since the displacement of the wedge-tool shows a spring-back for Δz_E at this stage. Therefore, this result suggests that the elastic deformation of the wire has little effect on the expansion of the adhered area.

Fig. 9 shows the relationship among the amplitude at the wedge-tool tip, the displacement of the wedge-tool, and the expansion of the adhered area measured simultaneously during ultrasonic bonding of Al wire with SiO_2 substrate under the condition of 1.0 W, 3.0 N. The adhered area increases rapidly by applying ultrasonic vibration at first and then gradually slows down. This is very similar to the displacement behavior of the wedge-tool. Therefore, the displacement of the wedge-tool can represent the adhered area formed by ultrasonic bonding. This knowledge is important, since the bond interfaces of practical electronic devices cannot be observed from the back of the substrates. On the other hand, the amplitude evolution of the wedge-tool tip is difficult to correlate with the adhered area expansion. For example, the amplitude shows a significant decrease at an ultrasonic vibration time of 30 ms. However, no significant change in the adhered area expansion behavior is observed.

4. Conclusions

The deformation behavior of Al wires during ultrasonic bonding to Al-Si, Si or SiO_2 substrates were investigated in detail by a laser displacement sensor, a laser Doppler vibrometer, and a high-speed video microscope. The following points became clear.

- (1) The deformation of the wire by applying the bonding force is completed immediately. Further deformation is induced by application of ultrasonic vibration.

- (2) The deformation induced by applying the bonding force consists of only an elastic component, whereas that by ultrasonic vibration consists of only a plastic component. The Al wire is not work-hardened by the plastic deformation during application of ultrasonic vibration.
- (3) The amount of deformation induced by ultrasonic vibration increases monotonously by increasing the ultrasonic power. On the other hand, it increases at first and then turns to decrease by increasing the bonding force, showing an appropriate bonding force to facilitate the wire deformation.
- (4) The adhered area expands in the direction perpendicular to the ultrasonic vibration.
- (5) The evolution of the wire deformation behavior and the expansion of the adhered area show an intimate correlation with each other.

References

- 1) G. G. Harman and J. Albers: IEEE Trans. Part. Hybrid. Packag. PHP-13 (1977) 406-412.
- 2) V. H. Winchell, II and H. M. Berg: IEEE Trans. Component. Hybrid. Manuf. Technol. CHMT-1 (1978) 211-219.
- 3) J. E. Krzanowski and N. Murdeshwar: J. Electron. Mater. 19 (1990) 919-928.
- 4) I. Lum, J. P. Jung and Y. Zhou: Metall. Mater. Trans. A 36A (2005) 1279-1286.
- 5) I. Lum, M. Mayer and Y. Zhou: J. Electron. Mater. 35 (2006) 433-442.
- 6) S. W. Or, H. L. W. Chan, V. C. Lo and C. W. Yuen: Sensor. Actuator. A 65 (1998) 69-75.
- 7) M. Mayer, O. Paul, D. Bolliger and H. Baltes: IEEE Trans. Component. Packag. Technol. 23 (2000) 393-398.
- 8) A. Shah, H. Gaul, M. Schneider-Ramelow, H. Reichl, M. Mayer and Y. Zhou: J. Appl. Phys. 106 (2009) 013503.